Cold Nuclear Effects on J/ψ and Υ Production in p+Pb Collisions at 5 TeV and Pb+Pb Collisions at 5.1 TeV

R. Vogt

Nuclear and Chemical Sciences Division,
Lawrence Livermore National Laboratory, Livermore, CA 94551, USA

Physics Department, University of California, Davis, CA 95616, USA

J/ψ and Υ Production

- $R_{p\mathrm{Pb}}(p_T)$ **at forward, backward, and midrapidity,** $R_{p\mathrm{Pb}}(y)$**, and forward/backward ratios** $R_{FB}(p_T)$ **and** $R_{FB}(y)$
  - **Central EPS09 compared to nDS(g), FGS-H, FGS-L and EKS98**
  - **LO vs NLO, EPS09 and nDS(g)**
  - **Mass and scale uncertainties on EPS09 NLO central set**
- $R_{\mathrm{PbPb}}(p_T)$ **at forward and midrapidity and** $R_{\mathrm{PbPb}}(y)$
- **Factorization of shadowing effects:** R_{PbPb} **at 5.1 TeV vs** $R_{p\mathrm{Pb}} \times R_{\mathrm{Pb}p}$ **at 5 TeV**

Quarkonium Calculation Based on Fitting $\sigma_{Q\overline{Q}}$

Caveat: full NNLO cross section unknown, could still be large corrections

Fit to subset of $Q\overline{Q}$ data to fix the factorization and renormalization scales for $m_c = 1.27$ GeV, lattice value at $m(3\,\mathrm{GeV})$, and $m_b = 4.65$ GeV, 1S mass: $(m_Q, \mu_F/m_Q, \mu_R/m_Q) = (1.27\,\mathrm{GeV}, 2.1^{+2.55}_{-0.85}, 1.6^{+0.11}_{-0.12})$, $(4.65\,\mathrm{GeV}, 1.4^{+0.75}_{-0.47}, 1.1^{+0.26}_{-0.19})$ with CT10 PDFs

Mass and scale uncertainty calculated with $m_c = 1.27 \pm 0.09$ GeV and $m_b = 4.65 \pm 0.09$ GeV; scale combinations $(\mu_F/m_q, \mu_R/m_Q) = (C, C)$, (C, L), (C, H), (L, C), (H, C), (L, L), and (H, H); (H, L) and (L, H) also checked; cross section extrema of mass and scale combinations added in quadrature to obtain uncertainty band

LHC $pp \to c\bar{c}$ at $\sqrt{s} = 2.76$ and 7 TeV not included in charm fit, 7 TeV $pp \to b\bar{b}$ included in bottom fit

Charm and bottom distributions agree with collinear factorization, even at LHC

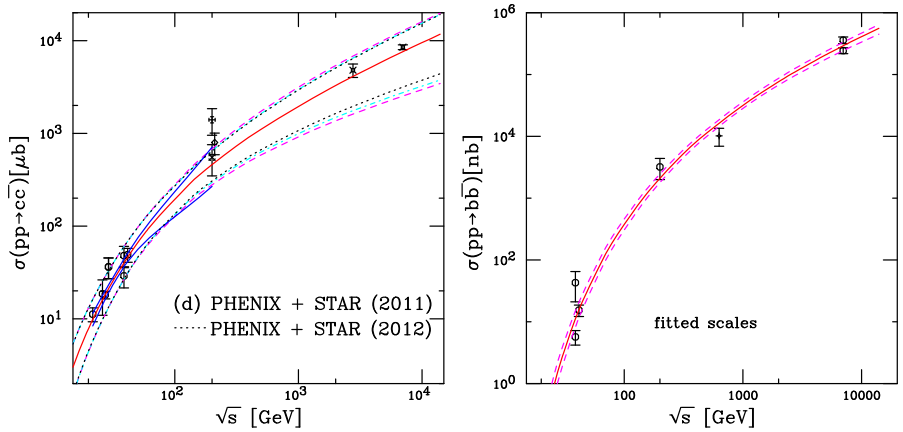

Figure 1: (Left) The energy dependence of the charm total cross section compared to data. The red curve is the best fit. The dashed magenta curves and dot-dashed cyan curves show the extent of the corresponding uncertainty bands. The dashed curves outline the most extreme limits of the band. (RV, R Nelson and A D Frawley, Phys. Rev. C **87** (2013) 014908.) (Right) The energy dependence of the bottom total cross section compared to data. The central value of the fit is given by the solid red curve while the dashed magenta curves show the corresponding uncertainty bands. (RV, R Nelson and A D Frawley, in progress)

Quarkonium Production Calculated in NLO CEM

In Color Evaporation Model (CEM) the quarkonium yield is a fraction of the total $Q\overline{Q}$ cross section below the heavy flavor meson pair threshold ($H\overline{H} \equiv D\overline{D}$, $B\overline{B}$)

$$\sigma_Q^{\rm CEM}(s_{_{NN}}) = F_Q \sum_{i,j} \int_{4m_Q^2}^{4m_H^2} d\hat{s} \int dx_1\, dx_2 \;\; f_i^p(x_1,\mu_F^2) \;\; f_j^p(x_2,\mu_F^2) \;\; \mathcal{J}(\hat{s})$$

Here $\mathcal{J}(\hat{s})$ is a kinematics-dependent Jacobian. At LO $\mathcal{J}(\hat{s}) = \delta(\hat{s} - x_1 x_2 s)/s$, at NLO and for differential cross sections, the expressions are more complex

The $Q\overline{Q}$ mass and scale parameters are used to calculate quarkonium production

Factor F_C fixed from a subset (low A) of J/ψ forward cross sections and F_B to summed Υ S state decays to dileptons at midrapidity for best fit mass and scale parameters

Same factor used for all mass and scale combinations to get uncertainty band

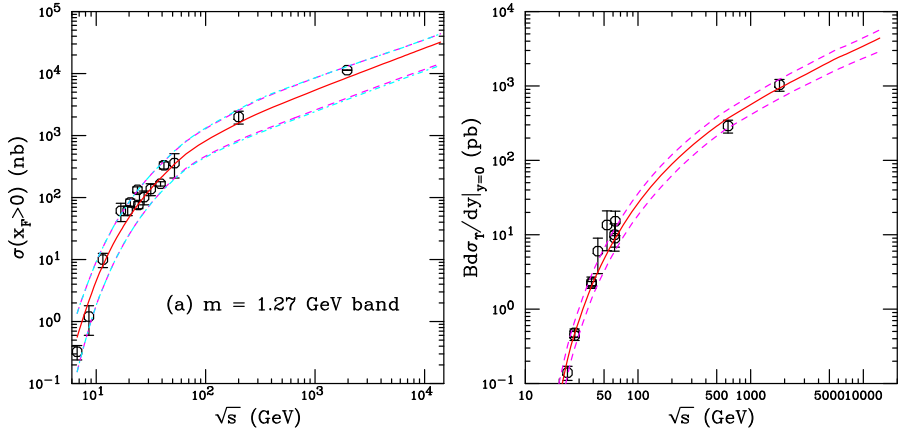

Figure 2: (Left) The energy dependence of the J/ψ forward cross section compared to data. The red curve is the best fit. The dashed magenta curves and dot-dashed cyan curves show the extent of the corresponding uncertainty bands. The dashed curves outline the most extreme limits of the band. (RV, R Nelson and A D Frawley, Phys. Rev. C **87** (2013) 014908.) (Right) The uncertainty band on the Υ cross section at $y = 0$. The central value of the fit in each case is given by the solid red curve while the dashed magenta curves show the corresponding uncertainty bands. (RV, R Nelson and A D Frawley, in progress)

Cold Nuclear Matter Effects in Hadroproduction

In heavy-ion collisions, one has to fold in cold matter effects, typically studied in pA or dA interactions from fixed-target energies to colliders

Hard probes, where production is calculable in QCD, are best to study differences between initial and final state effects

Important cold nuclear matter effects in hadroproduction include:

- **Initial-state nuclear effects on the parton densities (nPDFs)**
- **Initial- (or final-) state energy loss**
- **Final-state absorption on nucleons**
- **Final-state break up by comovers (hadrons or partons)**
- **Intrinsic $Q\overline{Q}$ pairs**

In this talk, I will concentrate on nuclear parton densities, not including any other effect

Nuclear Gluon PDFs at NLO

EPS09 NLO and EKS98 (LO) very similar for $x > 0.002$ with significant antishadowing, nDS(g) NLO has almost none

nDSg and EKS98 have stronger shadowing than central EPS09 at low x, FGS-H(L) strongest but valid only for $x > 10^{-5}$

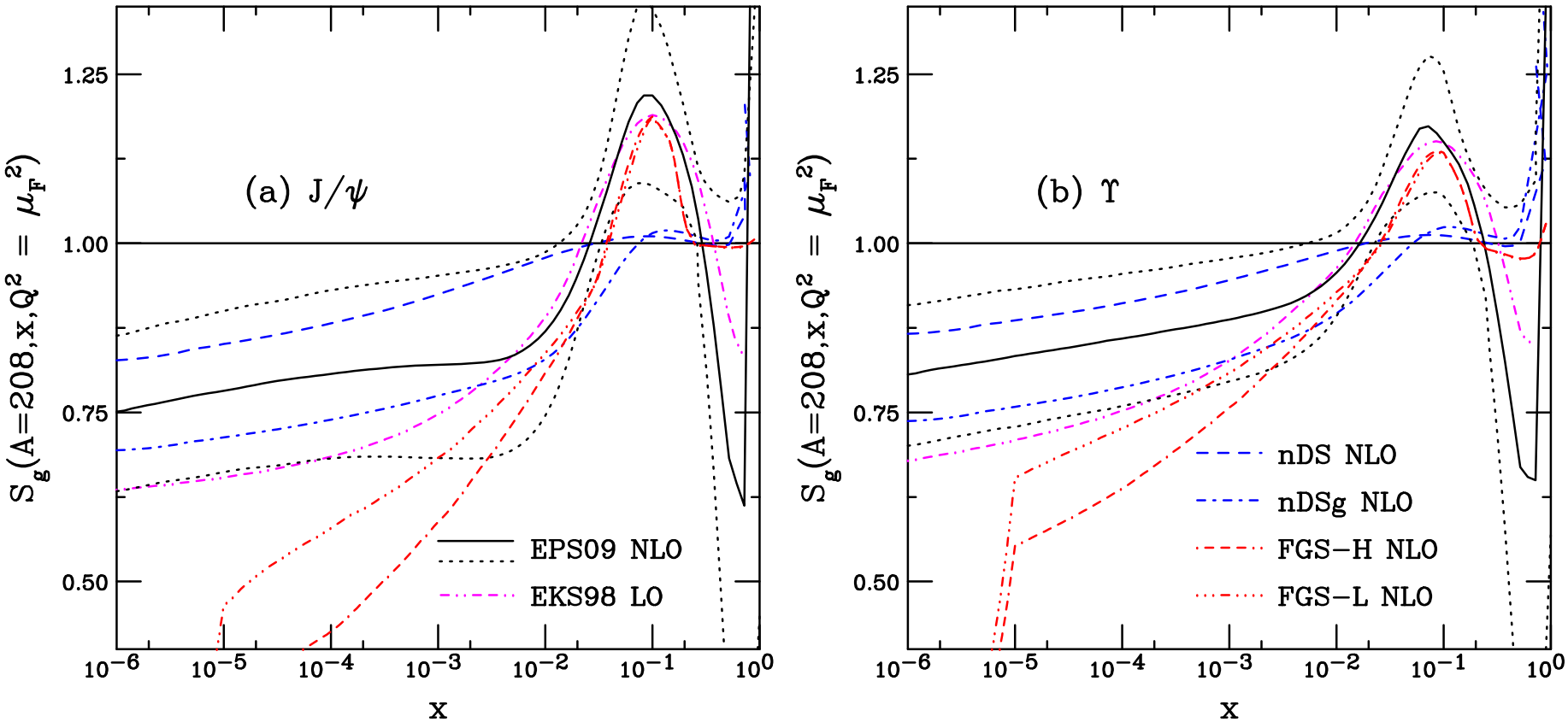

Figure 3: **Gluon shadowing ratios calculated for Pb nuclei ($A = 208$) calculated at the central value of the fitted factorization scales for J/psi (a) and ϒ (b). The EPS09 NLO set is shown by the black solid curve while the uncertainty band is outlined by the black dotted curves. The NLO nDS and nDSg parameterizations are given in the blue dashed and dot-dashed curves respectively. The LO EKS98 parameterization is given in the magenta dot-dot-dash-dashed curve. The NLO FGS-H and FGS-L results are given by the red dot-dash-dash-dashed and dot-dot-dot-dashed curves respectively.**

Comparison of nPDF Results I: $R_{p\mathrm{Pb}}(p_T)$

Central EPS09 NLO set compared to nDS NLO, nDSg NLO and EKS98 (LO)

nDS effect is weakest of all while nDSg is weak at backward rapidity but stronger than EPS09 at mid- and forward rapidity

EKS98 and EPS09 NLO are very similar for $x > 0.01$ so they agree well at backward and mid-rapidity while EKS98 is stronger at forward rapidity

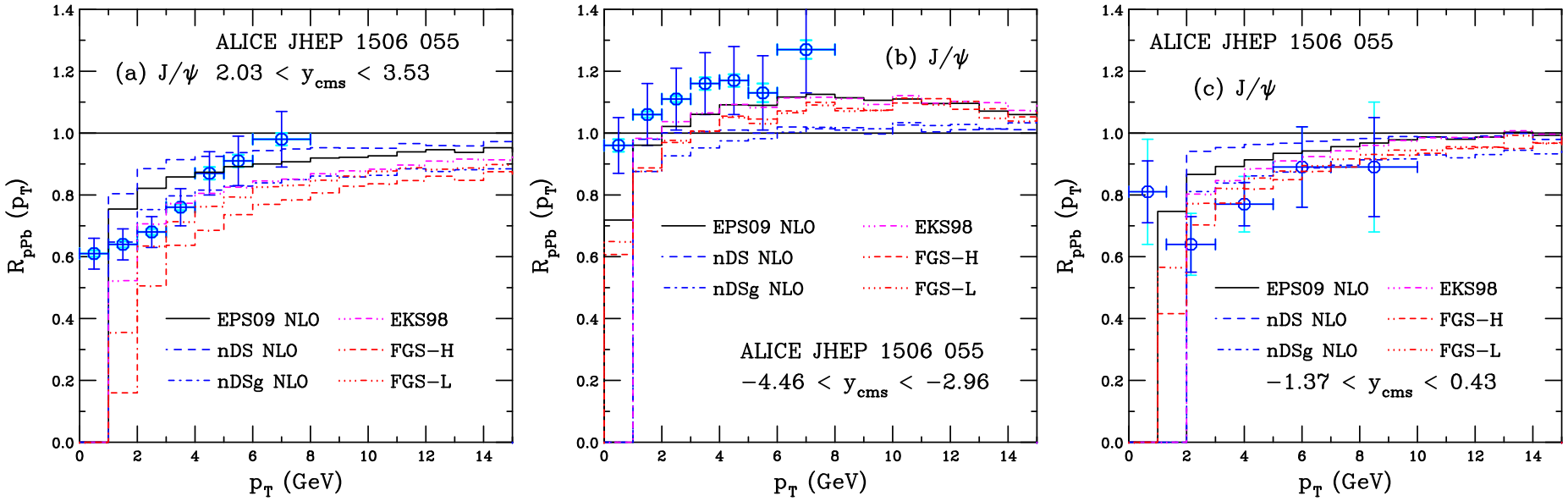

Figure 4: **The ratio $R_{p\mathrm{Pb}}(p_T)$ for ALICE at forward (left), backward (center) and mid- (right) rapidity. The results are shown for central EPS09 NLO (black), nDS NLO (blue dashed), nDSg NLO (blue dot-dashed) and EKS98 LO (magenta dot-dot-dash-dashed), FGS-H (red dot-dash-dash-dashed) and FGS-L (red dot-dot-dot-dash).**

Comparison of nPDF Results II: $R_{p\mathrm{Pb}}(y)$

EKS98 LO follows EPS09 NLO central set until $y > -2$ where it decreases linearly while EPS09 becomes flatter

EPS09 abrupt change of slope near antishadowing region follows from the gluon shadowing ratio, almost like the low x behavior had to join to assumed antishadowing shape at intermediate x

nDS and nDSg, with no antishadowing, have a weaker y dependence overall

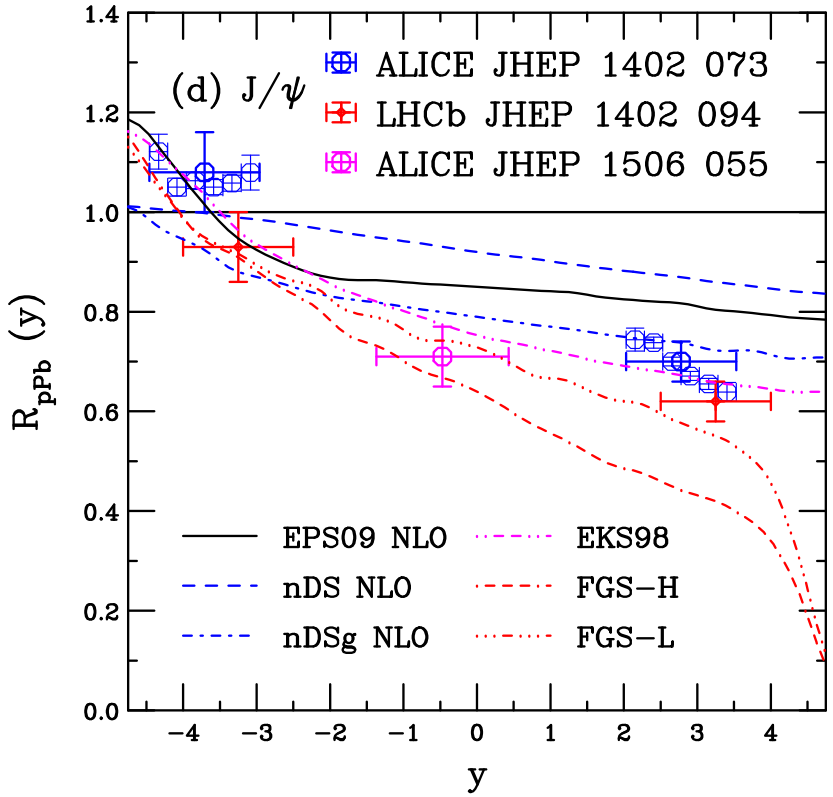

Figure 5: **The $R_{p\mathrm{Pb}}(y)$ for J/ψ production measured by ALICE and LHCb is compared to calculations. The results are shown for central EPS09 NLO (black), nDS NLO (blue dashed), nDSg NLO (blue dot-dashed) and EKS98 LO (magenta dot-dot-dash-dashed), FGS-H (red dot-dash-dash-dashed) and FGS-L (red dot-dot-dot-dash).**

Comparison of nPDF Results III: R_{FB}

nDS has strongest p_T dependence of $R_{FB}(p_T)$, EKS98 comes closest to agreement with low p_T data due to the stronger effect at low x than EPS09

Only EPS09 shows curvature in $R_{FB}(y)$, the others show an almost linear y dependence

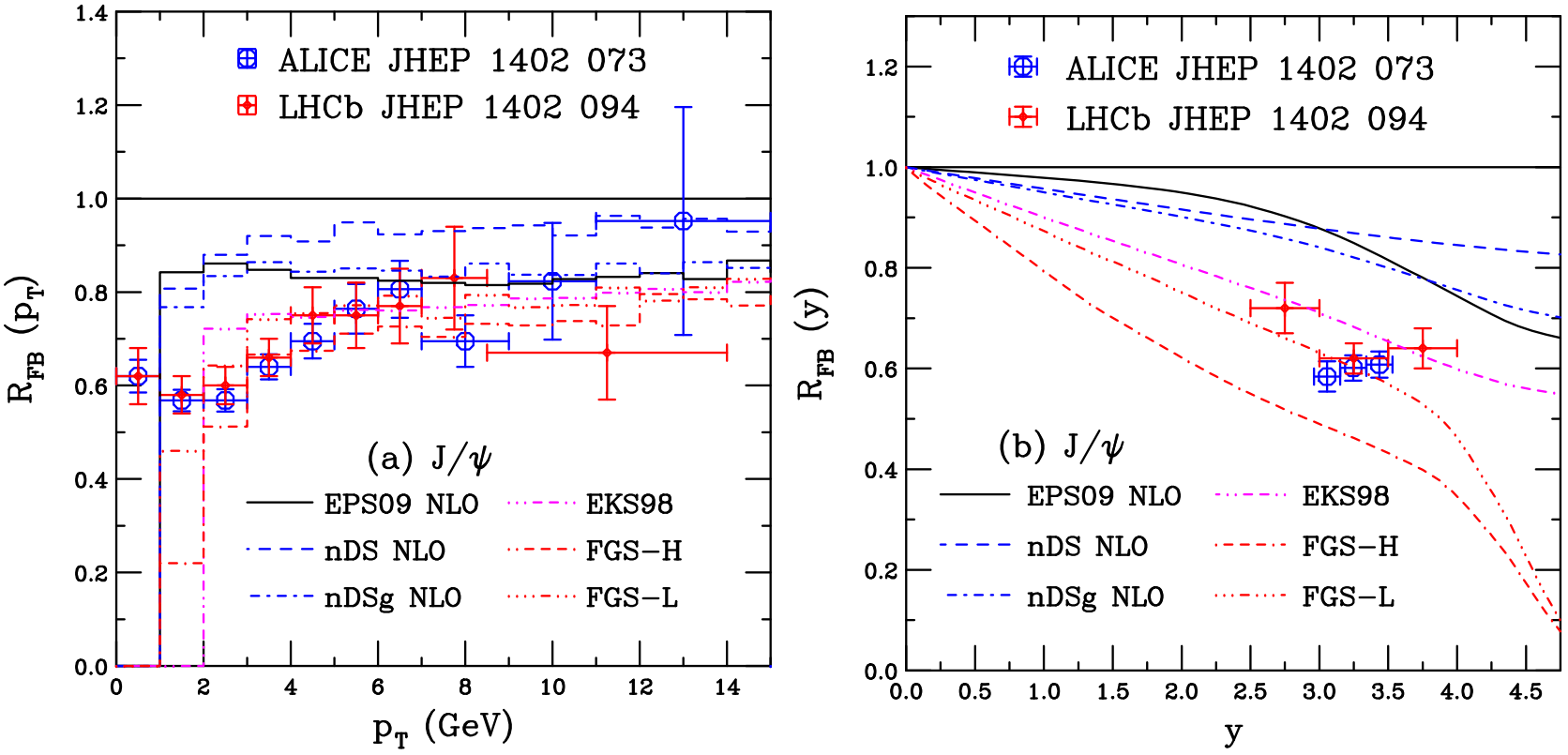

Figure 6: **The ratio R_{FB} as a function of p_T (left) and rapidity (right) for J/ψ compared to the ALICE and LHCb data. The results are shown for central EPS09 NLO (black), nDS NLO (blue dashed), nDSg NLO (blue dot-dashed) and EKS98 LO (magenta dot-dot-dash-dashed), FGS-H (red dot-dash-dash-dashed) and FGS-L (red dot-dot-dot-dash).**

Comparison of nPDF Results IV: Υ $R_{p\mathrm{Pb}}(y)$, $R_{FB}(y)$

Generally relatively good agreement with $R_{p\mathrm{Pb}}$

Rather narrow antishadowing band for FGS sets

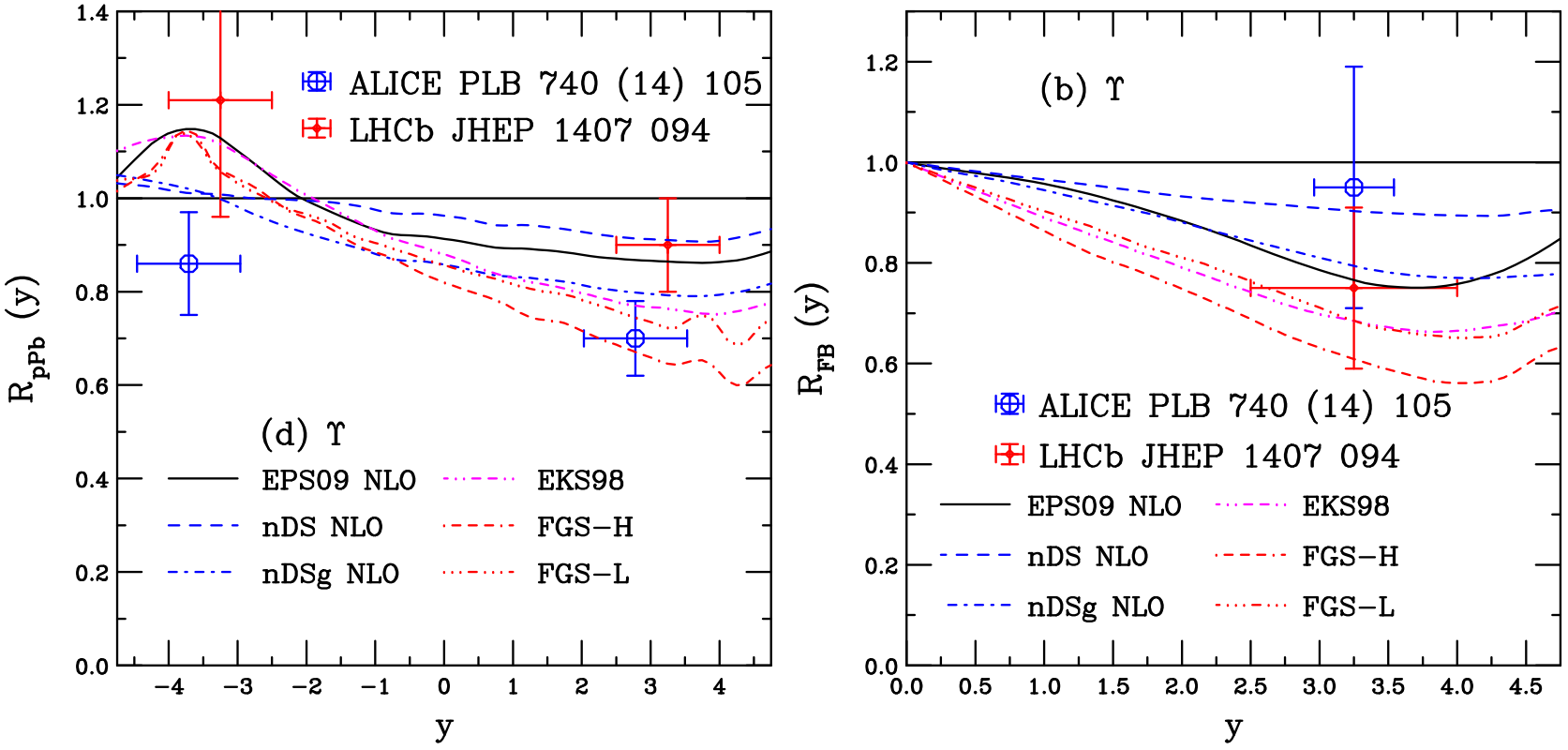

Figure 7: **The ratio $R_{p\mathrm{Pb}}(y)$ (left) and $R_{FB}(y)$ (right) for Υ production compared to the ALICE and LHCb data. The results are shown for central EPS09 NLO (black), nDS NLO (blue dashed), nDSg NLO (blue dot-dashed) and EKS98 LO (magenta dot-dot-dash-dashed), FGS-H (red dot-dash-dash-dashed) and FGS-L (red dot-dot-dot-dash).**

NLO vs LO: EPS09

The nPDF set should be appropriate to the order of the calculation: if using the LO set in a NLO calculation agrees better with the data, it isn't really better

NLO calculation required for CEM p_T distribution and is more appropriate

LO CEM uncertainty band is broader, with stronger shadowing, to counterbalance the flatter low x behavior of CTEQ61L while CTEQ6M is valence-like: different behavior of proton PDFs makes good order-by-order agreement of $R_{p\mathrm{Pb}}$ difficult

Starting scale of EPS09 is 1.69 GeV^2, same as CTEQ6 starting scale

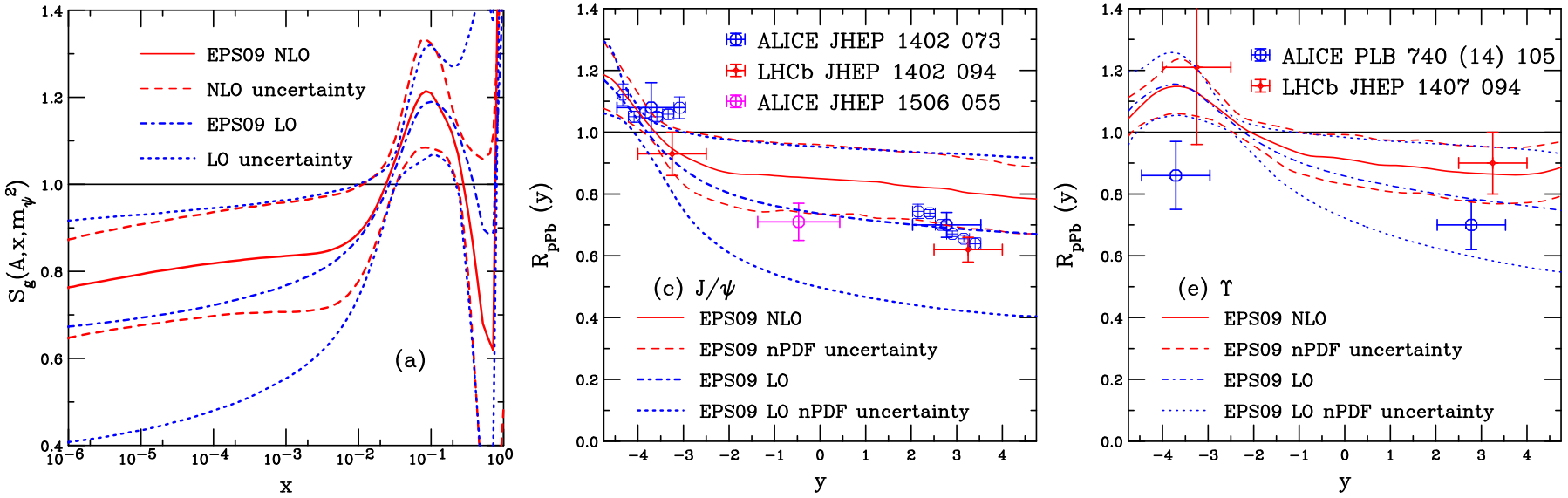

Figure 8: **(Left) The EPS09 LO (blue) and NLO (red) uncertainty bands for gluon shadowing. The corresponding uncertainty bands for $R_{p\mathrm{Pb}}(y)$ at $\sqrt{s_{NN}} = 5$ TeV for J/ψ (center) and Υ (right).**

NLO vs LO: nDS

While there are some differences between the LO and NLO nDS and nDSg ratios, especially for nDSg at $x \sim 0.01$, the LO and NLO ratios are much closer than those of the EPS09 central sets, here order of calculation is not an issue

nDS(g) employs GRV98 LO and NLO proton PDFs, the Q^2 range of the nPDF, $1 < Q^2 < 10^6$ GeV^2, is above the minimum scale of GRV98, unlike EPS09 with CTEQ6

LO nPDF set EKS98 gives same result within 2-3% in LO and NLO CEM calculations

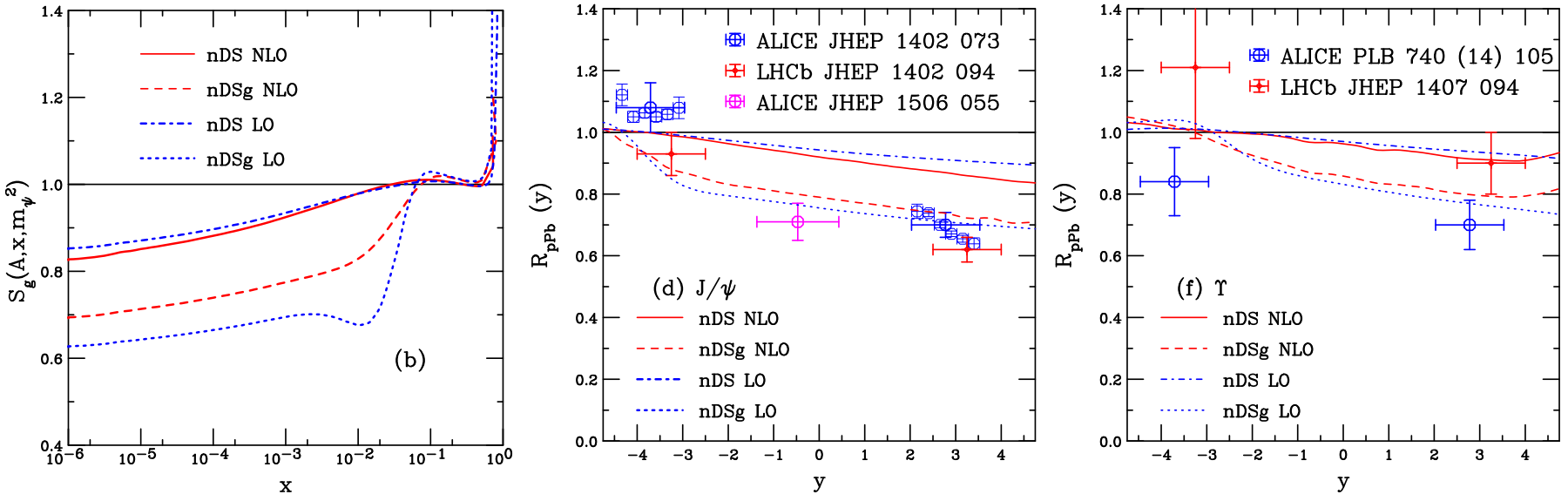

Figure 9: **(Left) The nDS and nDSg LO (blue) and NLO (red) gluon shadowing ratios. The corresponding results for $R_{p\mathrm{Pb}}(y)$ at $\sqrt{s_{NN}} = 5$ TeV are shown for J/ψ (center) and Υ (right).**

Calculating Mass and Scale Uncertainties

We calculate the mass and scale uncertainties in 3 ways:

The first two follow Cacciari, Nason and RV where the cross section extremes with mass and scale are used to calculate the uncertainty

$$\sigma_{\rm max} = \sigma_{\rm cent} + \sqrt{(\sigma_{\mu,\rm max} - \sigma_{\rm cent})^2 + (\sigma_{m,\rm max} - \sigma_{\rm cent})^2} \ ,$$
$$\sigma_{\rm min} = \sigma_{\rm cent} - \sqrt{(\sigma_{\mu,\rm min} - \sigma_{\rm cent})^2 + (\sigma_{m,\rm min} - \sigma_{\rm cent})^2} \ ,$$

$m/\mu_F/\mu_R$ **v1 We take the ratios of p+Pb to pp for each mass and scale combination and then locate the extrema in each case – this gives the uncertainty on $R_{p\rm Pb}$ of each set, can appear odd if ratios are not very different but the extrema changes between sets (as it does for $R_{p\rm Pb}(y)$)**

$m/\mu_F/\mu_R$ **v2 We locate the mass and scale extrema and calculate the uncertainty as above and then form $R_{p\rm Pb}$ by dividing by the pp cross section calculated with the central parameter set – this forms global $R_{p\rm Pb}$ based on the cross sections rather than the shadowing ratios and is thus significantly larger, especially at low p_T, becoming smaller at high p_T (Does not apply to R_{FB})**

$m/\mu_F/\mu_R$ **v3 We add the mass and scale uncertainties in quadrature, a la EPS09, and then form $R_{p\rm Pb}$ by dividing by the central pp cross section – since this is a cumulative uncertainty rather than based on the greatest excursion from the mean, it is the largest uncertainty at low p_T. This was calculated assuming that the appropriate μ_F/m and μ_R/m pairs are $[(H,H),(L,L)]$, $[(H,C),(L,C)]$ and $[(C,H),(C,L)]$, other choices could lead to different results**

Mass and Scale Uncertainty on $d\sigma/dp_T$

Mass and scale uncertainty bands give good agreement with p+Pb data for $p_T > 2$ GeV in all rapidity regions, best agrement with central result for $p_T > 5$ GeV

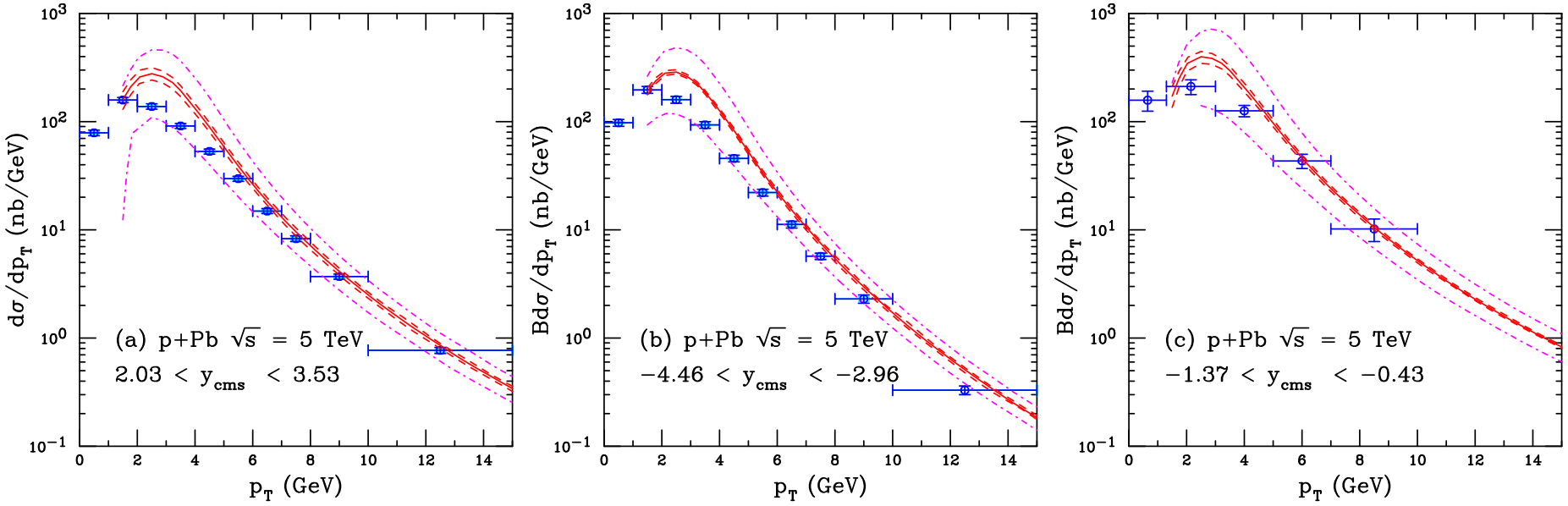

Figure 10: **The ALICE J/ψ p_T distributions at forward (a), backward (b) and midrapidity (c) at NLO in the CEM [?]. The solid red curve is the EPS09 NLO central value while the dashed red curves are the EPS09 NLO uncertainties and the dot-dashed magenta curves are the mass and scale uncertainties.**

Mass and Scale Uncertainty Bands I: $R_{p\mathrm{Pb}}(p_T)$

Uncertainties based on the differences due to EPS09 NLO alone, *i.e.* taking the extrema based on the ratios, gives very small uncertainty, smaller than EPS09 NLO

Uncertainties based on cross sections are much larger with v3 bigger than v2 at low p_T, expected since ratio is cumulative

Ratios decrease at high p_T where the scale choices are less important since $p_T \gg m$

Υ uncertainties narrower than J/ψ

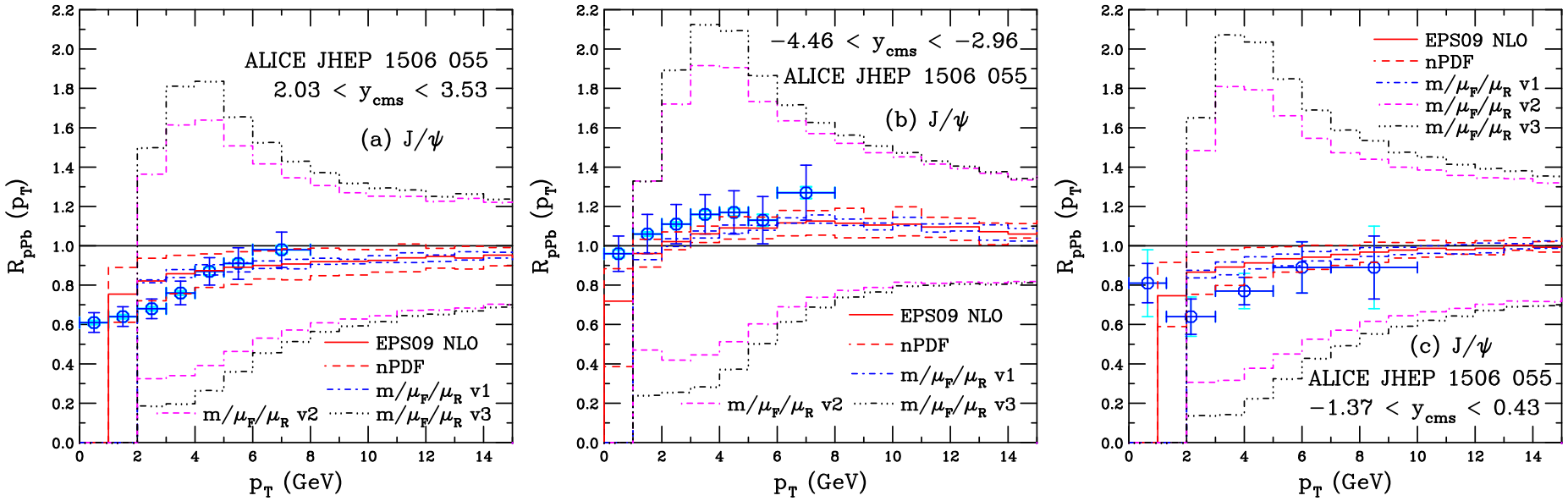

Figure 11: **The mass and scale uncertainties in the ratio $R_{p\mathrm{Pb}}(p_T)$ are compared to those for EPS09 NLO alone for ALICE at forward (left), backward (middle) and mid- (right) rapidity. The EPS09 uncertainty band is shown in red while the uncertainties calculated with method v1 in blue, v2 in magenta and v3 in black.**

Mass and Scale Uncertainty Bands II: $R_{p\mathrm{Pb}}(y)$

Rapidity dependence with v1 exhibits the perils(?) of basing extrema on individual $R_{p\mathrm{Pb}}$ ratios – when one ratio is larger at high $|y|$ but not at midrapidity, the calculated v1 changes slope at the switching point

Right-hand plot indicates how this happens, the ratio with (H, H) is larger than that of the next highest ratio, that with (C, L) except for $|y| < 2$

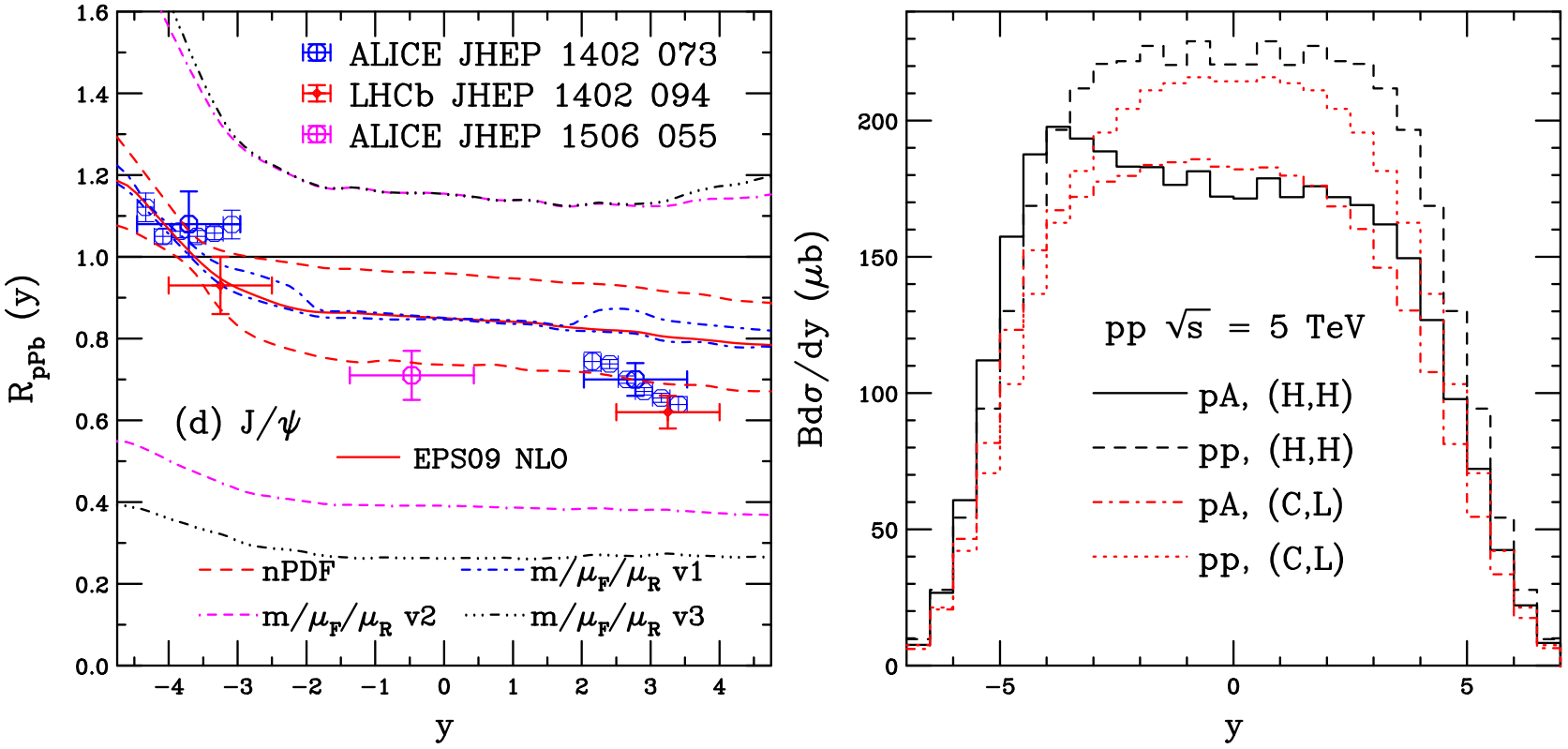

Figure 12: **(Left) The mass and scale uncertainties in the ratio $R_{p\mathrm{Pb}}(y)$ are compared to those for EPS09 NLO alone. The EPS09 uncertainty band is shown in red while the uncertainties calculated with method v1 in blue, v2 in magenta and v3 in black. (Right) The pp and p+Pb rapidity distributions for the (H, H) (C, L) sets showing the differences leading to the change in the upper limit of the mass and scale uncertainties of method v1 around midrapidity.**

Mass and Scale Uncertainty Bands III: R_{FB}

Only v1 and v3 apply here (v2 is equivalent to v1 in this case)

Taking the forward to backward ratio before calculating the uncertainty band makes this ratio essentially insensitive to the mass and scale

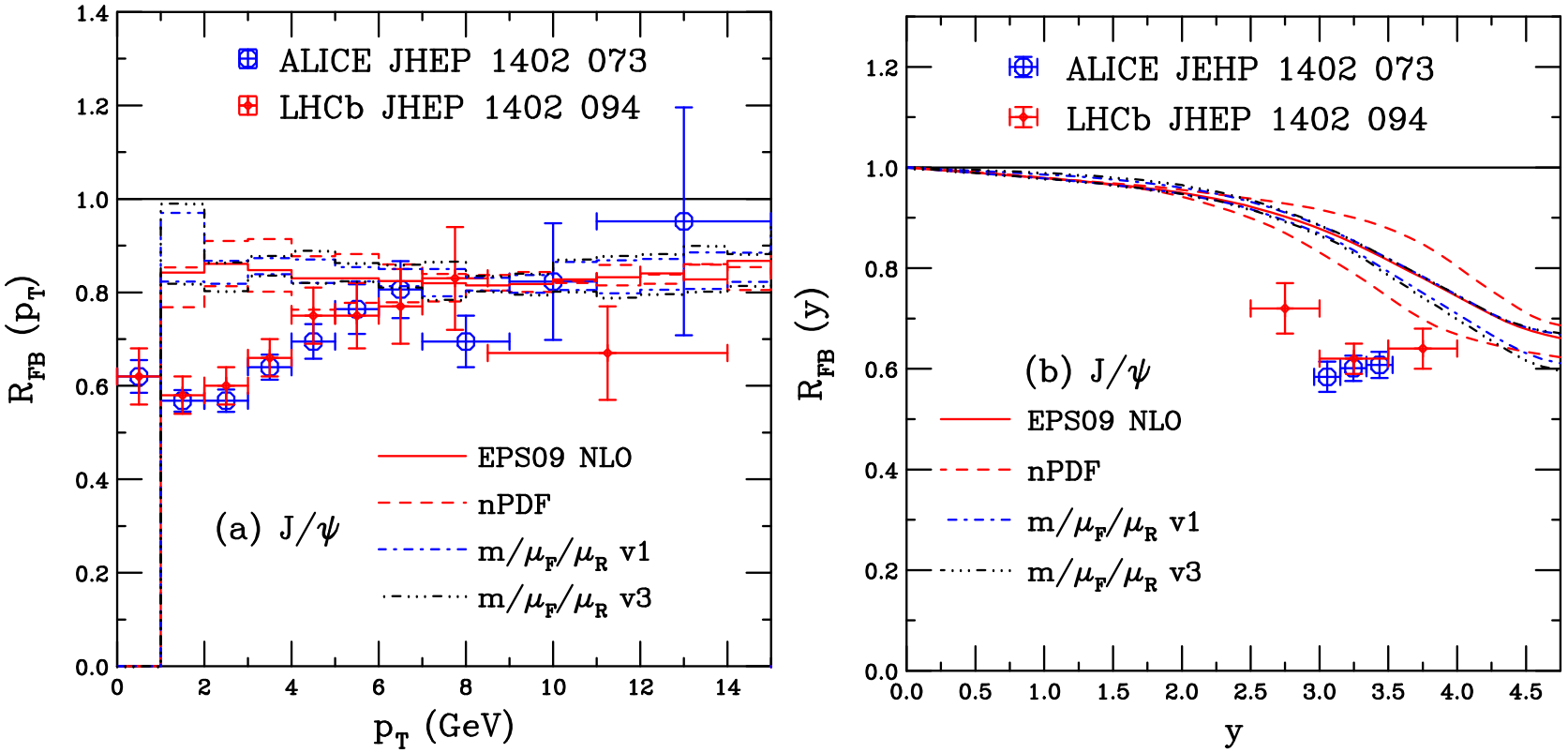

Figure 13: **The mass and scale uncertainties in the ratios $R_{FB}(p_T)$ (left) and $R_{FB}(y)$ (right) are compared to those for EPS09 NLO alone for ALICE at forward (left), backward (middle) and mid- (right) rapidity. The EPS09 uncertainty band is shown in red while the uncertainties calculated with method v1 are in blue and those with v3 are in black.**

Mass and Scale Uncertainty Bands IV: Υ $R_{p\mathrm{Pb}}(y)$, $R_{FB}(y)$

$R_{p\mathrm{Pb}}(y)$ band is narrower than for J/ψ, $R_{FB}(y)$ is wider because $R_{p\mathrm{Pb}}(y)$ is more regular

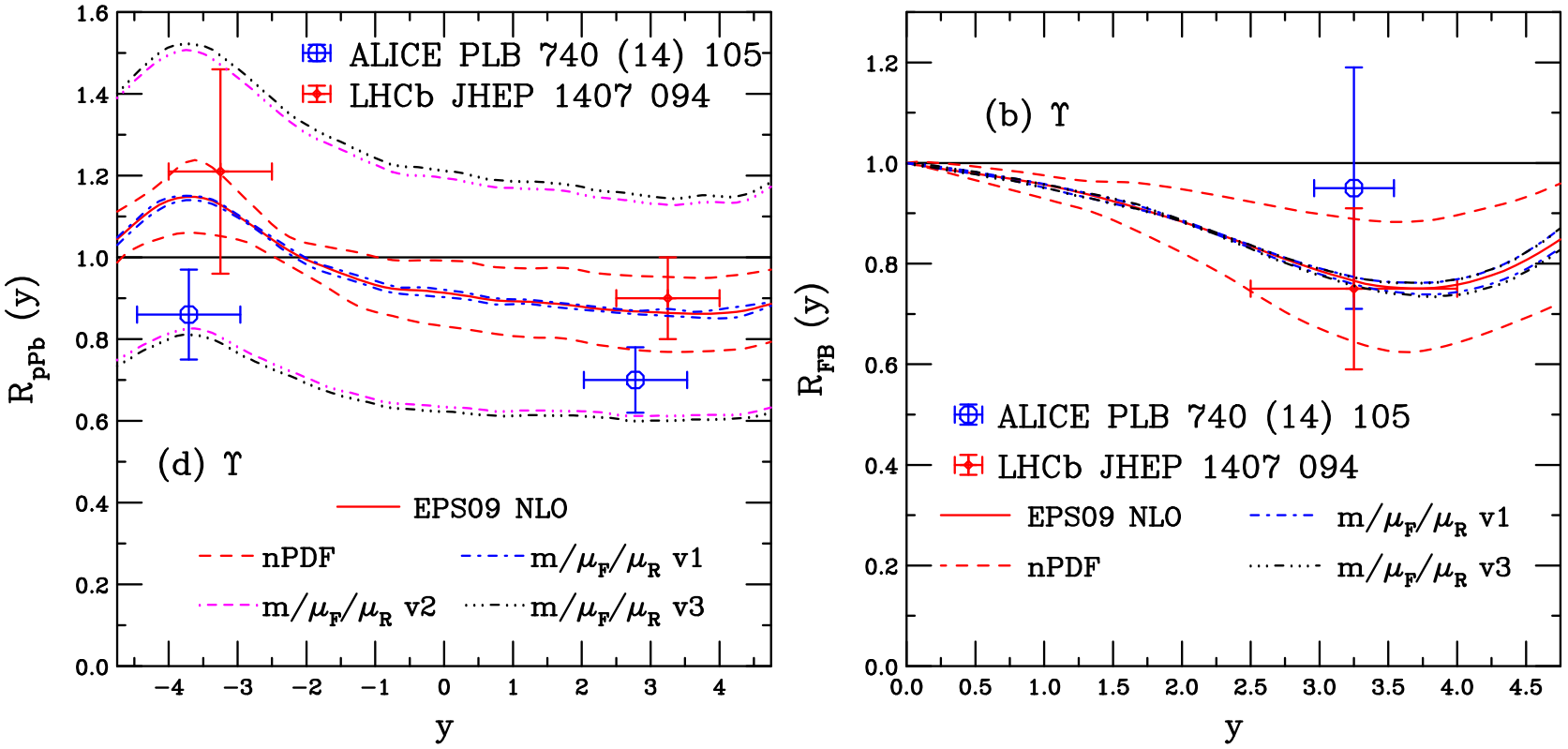

Figure 14: **The mass and scale uncertainties in the ratios $R_{p\mathrm{Pb}}(y)$ (left) and $R_{FB}(y)$ (right) are compared to those for EPS09 NLO alone for ALICE and LHCb. The EPS09 uncertainty band is shown in red while the uncertainties calculated with method v1 are in blue, v2 are in magenta and v3 are in black.**

Predictions for J/ψ in Pb+Pb Collisions at 5.1 TeV

p_T dependence stronger at midrapidity, effectively square of central rapidity p+Pb ratio, forward p_T-dependent ratio is flatter, product of shadowing and antishadowing ratios

$R_{\rm PbPb}(y)$ symmetric around midrapidity, p_T-integrated ratio is less than unity at all y with stronger effect at midrapidity than forward rapidity – coalescence production would build up R_{AA} at midrapidity, leaving a suppression factor less dependent upon rapidity

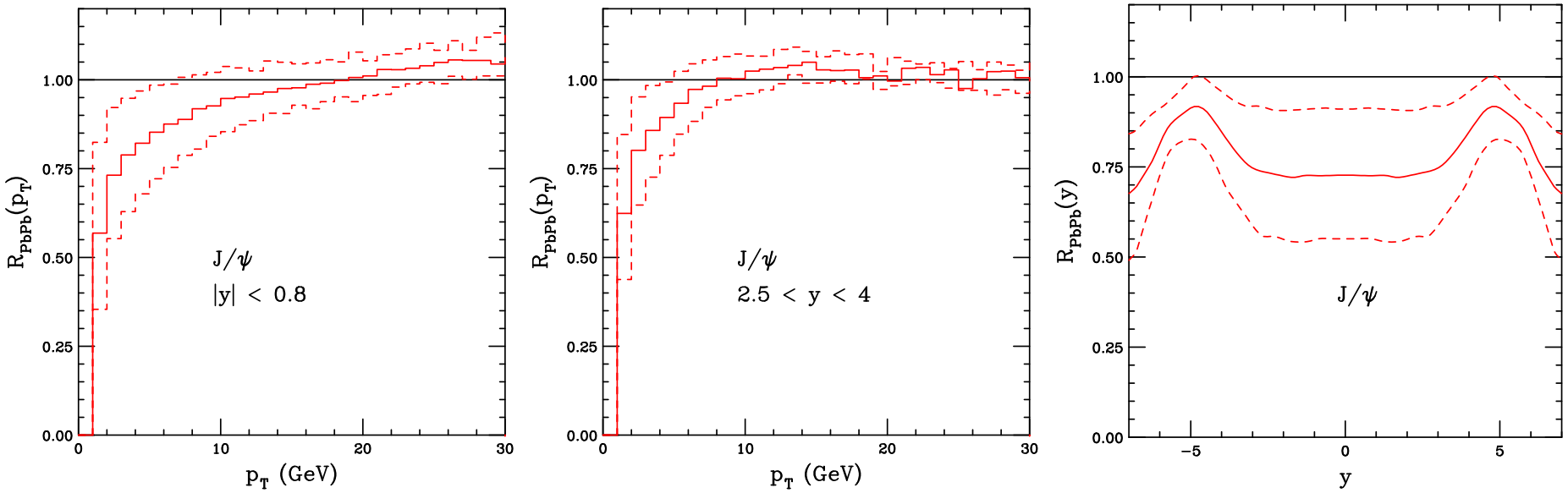

Figure 15: **The EPS09 NLO uncertainty band as a function of p_T for mid (left) and forward (center) rapidities and as a function of y, integrated over all p_T (right).**

Predictions for Υ in Pb+Pb Collisions at 5.1 TeV

Similar behavior observed for Υ as for J/ψ but effect is weaker overall, especially for forward rapidity

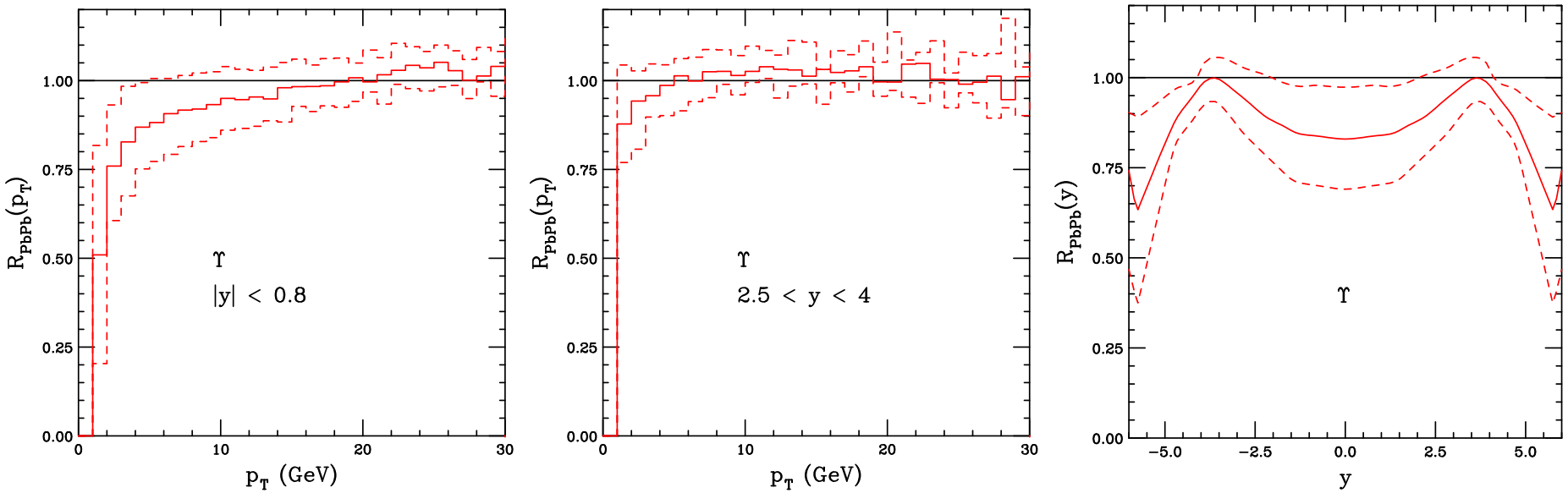

Figure 16: **The EPS09 NLO uncertainty band as a function of p_T for mid (left) and forward (center) rapidities and as a function of y, integrated over all p_T (right).**

Predicting $R_{\rm PbPb}$ at 5.1 TeV from $R_{p\rm Pb}$ at 5 TeV: J/ψ

The factorization is exact for the CEM at LO because the process is $2 \to 1$ and the scale is fixed ($p_T = 0$) so x_1 and x_2 are known at each y

Factorization is not automatic at NLO because process is $2 \to 2\,[(c\overline{c}) + g/q/\overline{q}]$ and the additional parton makes the correspondence between x_1, x_2 and y inexact, even at fixed rapidity – agreement is good, nevertheless

Works well for 2.76 TeV, is a bit off for p_T at higher energy because of rapidity mismatch (effect of energy difference is small for J/ψ)

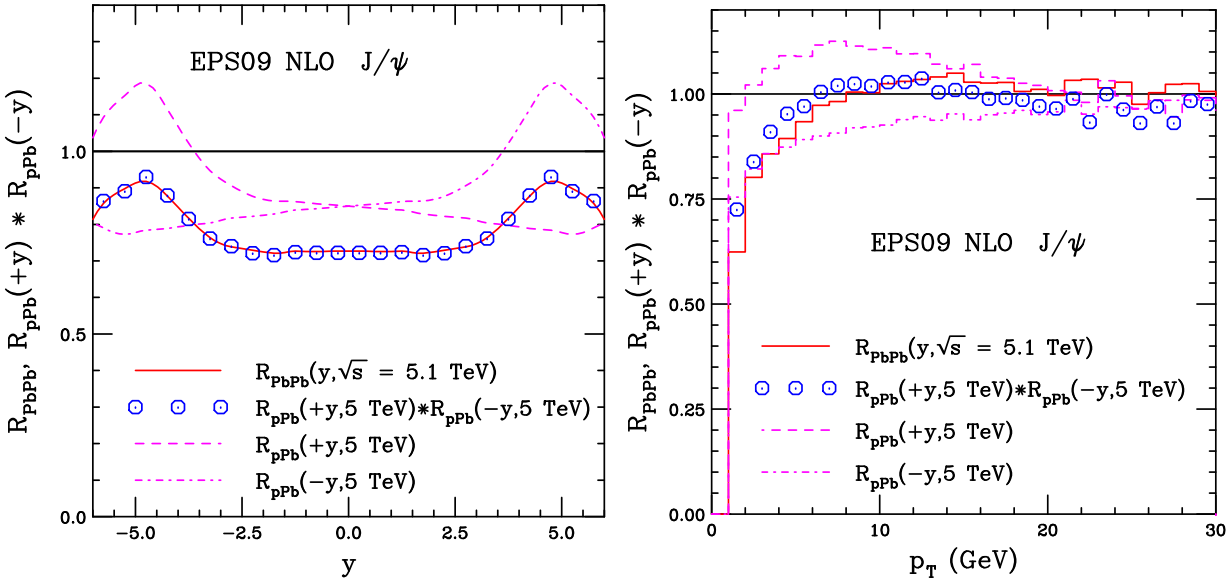

Figure 17: **The R_{AA} (red) ratio is compared to the product $R_{pA}(+y) \times R_{pA}(-y)$ (points) along with the individual pA ratios at forward (dashed) and backward (dot-dashed) rapidity. Results are compared for the rapidity distributions at LO (left) and NLO (middle) as well as for the p_T dependence at NLO (right).**

Predicting $R_{\rm PbPb}$ at 5.1 TeV from $R_{p\rm Pb}$ at 5 TeV: Υ

Rapidity mismatch is a smaller effect for Υ but energy difference is more important for large rapidities where Υ production runs out of phase space sooner for p+Pb collisions

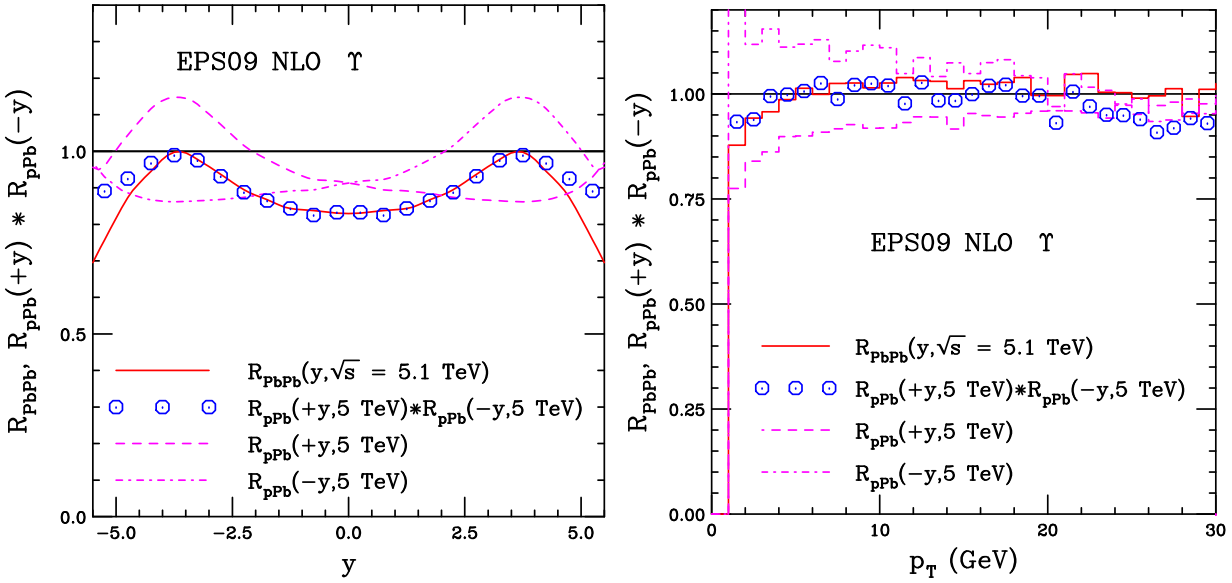

Figure 18: **The R_{AA} (red) ratio is compared to the product $R_{pA}(+y)\times R_{pA}(-y)$ (points) along with the individual pA ratios at forward (dashed) and backward (dot-dashed) rapidity. Results are compared for the rapidity distributions at LO (left) and NLO (middle) as well as for the p_T dependence at NLO (right).**

Summary

- Fitting the scale parameters to the total $Q\overline{Q}$ cross section data significantly reduces the uncertainties on open heavy flavor and quarkonium production
- Differences in LO and NLO results for EPS09 on J/ψ production illustrates the fact that gluon nPDF is still not very well constrained, although, given the approximate concordance of the nDS results, the EPS09 discrepancy may be due to the choice of CTEQ6 proton PDFs
- Best results are with oldest, LO only set, EKS98, similar to EPS09 LO, new global analysis needed that includes LHC data
- Many caveats on medium effects, *e.g.* initial and/or final state energy loss, production mechanism, saturation effects – while the $R_{p\mathrm{Pb}}$ results, both as a function of p_T and y, look good, the R_{FB} results are not as good: pp data at 5 TeV are required
- p+Pb data at 5 TeV can be used to estimate the expected effect in Pb+Pb collisions at 5.1 TeV, calculations at 5 TeV are good estimate of effect at 5.1 TeV as well